

Non-Uniform Pressure Universes: The Hubble Diagram of Type Ia Supernovae and the Age of the Universe

Mariusz P. Dąbrowski,^{1,2} and Martin A. Hendry,^{2,3}

¹*Institute of Physics, University of Szczecin, Wielkopolska 15, 70-451 Szczecin, Poland*

²*Astronomy Centre, University of Sussex, Falmer, Brighton BN1 9QH, UK*

³*Dept of Physics and Astronomy, University of Glasgow, Glasgow G12 8QQ, UK*

Accepted —. Received —; in original form 2 December 2024

ABSTRACT

We use the redshift-magnitude relation, as derived by Dąbrowski (1995), for the two exact non-uniform pressure spherically symmetric Stephani universes to test the agreement of these models with recent observations of high redshift type Ia supernovae (SNIa), as reported in Perlmutter et al. (1997). By a particular choice of model parameters, we show that these models can give an excellent fit to the observed redshifts and (corrected) B band apparent magnitudes of the Perlmutter et al. data, but for an age of the Universe which is typically about two Gyr – and may be more than three Gyr – greater than in the corresponding Friedmann model, for which positive values of the deceleration parameter appear to be favoured by the data. We show that this age increase is obtained for a wide range of parameter values, and depends only on the ratio of two parameters of the Stephani model.

Several recent calibrations of the Hubble parameter, from the Hubble diagram of SNIa and other distance indicators, indicate a value of $H_0 \simeq 65$, and a Hubble time of ~ 15 Gyr. Based on this value for H_0 and assuming $\Lambda \geq 0$, the P97 data would imply a Friedmann age of at most 13 Gyr and in fact a best-fit (for $q_0 = 0.5$) age of only 10 Gyr. Our Stephani models, on the other hand, can give a good fit to the P97 data with an age of up to 15 Gyr, and a best-fit value of 13 Gyr. The Stephani models considered here could, therefore, significantly alleviate the conflict between recent cosmological and astrophysical age predictions.

Key words: cosmology: large-scale structure of Universe - relativity

1 INTRODUCTION

The standard isotropic Friedmann cosmological models have naturally been the most widely investigated models in studies of the large-scale structure of the Universe. This is hardly surprising, in view of their mathematical simplicity and their generic prediction of an approximately linear Hubble expansion at low redshift, which is in excellent agreement with observational data (c.f. Strauss & Willick 1995; Postman 1997). Even in Friedmann models, however, the relation between apparent magnitude and log redshift is in general non-linear at higher redshift and depends explicitly on the spatial curvature of the Universe – or equivalently on the deceleration parameter, q_0 .

For several decades astronomers have attempted to use the Hubble diagram of some suitable ‘standard candle’ (e.g. first-ranked cluster galaxies) to place constraints on the global geometry of the universe by comparing the observed redshift-magnitude relation of the standard candle with that predicted in Friedmann models with different values of q_0

(c.f. Peach 1970; Gunn & Oke 1975; Schneider, Gunn & Hoessel 1983; Sandage 1988). Results from such analyses have thus far proved inconclusive, however. Due to the intrinsic dispersion in the luminosity function of a typical standard candle, one must reach at least $z \simeq 1$ before the predictions of models with different values of q_0 become sufficiently distinct to be detectable; at the same time, however, the effects of luminosity and number density evolution also become important at these redshifts, and are very difficult to correct for. The situation for the Hubble diagram of quasars is equally – if not even more – problematical. Tonry (1993) suggested that the constraints on q_0 from such studies were no better than $-1 < q_0 < 1$.

Recently, however, it has been suggested that type Ia supernovae (hereafter SNIa) represent a standard candle of sufficiently small dispersion to allow meaningful estimates of q_0 to be derived from the SNIa Hubble diagram at high redshift. In Perlmutter et al. (1997; hereafter P97) a preliminary analysis is presented of seven distant SNIa in the range $0.35 < z < 0.50$. A comparison of the SNIa magnitudes and

redshifts with the predicted relation for various Friedmann models appears to favour positive values of q_0 , and is best fitted by values close to $q_0 = 0.5$. This poses a potentially serious problem for Friedmann models. Since many recent determinations of the Hubble constant (including several analyses using SNIa) suggest that H_0 lies in the range 65–70, this would imply an age of the universe of less than 10 Gyr in the ‘standard’ $\Omega_0 = 1, \Lambda_0 = 0$ scenario. This result would appear to be in sharp conflict with recent astrophysical age determinations from e.g. globular clusters and white dwarf cooling (c.f. Chaboyer 1995; Hendry & Tayler 1996). Reducing the value of Ω_0 lessens the conflict somewhat, but agreement is still only marginal if one accepts a robust lower bound for the matter density of $\Omega_m = 0.3$, as has been suggested by several different methods of analysing large-scale galaxy redshift surveys (c.f. Strauss & Willick 1995). This situation has helped to give a renewed impetus to models with a positive cosmological constant (c.f. Liddle et al. 1996) which contributes an additional component, Ω_Λ , to make up the critical density and at the same time extends the age of the Universe by up to 2 Gyr – depending on the value of H_0 and Ω_m . However, because of the relation

$$q_0 = \frac{1}{2}\Omega_m - \Omega_\Lambda, \quad (1)$$

it is clear that a positive value of q_0 is incompatible with a positive value of Λ_0 unless the matter density is at least two-thirds of the critical density. The $q_0 = 0$ case, assuming $\Omega_m = 2/3$, $\Omega_\Lambda = 1/3$ and $H_0 = 65$, would give an age of the Universe of just over 11 Gyr; as q_0 increases the age is decreased still further. Thus, if the preliminary results of P97 prove to be correct and the deceleration parameter is positive, then the conflict between cosmological and astrophysical age predictions remains firmly unresolved.

In this paper we propose one method to alleviate this conflict by considering some inhomogeneous cosmological models in which the relation between the age of the Universe and a generalised Hubble constant is more general than in the Friedmann case. In particular, we show that this allows us to achieve a very good fit between the predicted redshift-magnitude relation and P97 data, but for an age of the Universe which is several Gyr older than in the Friedmann case. The models under consideration have been discussed before and are known as Stephani Universes (c.f. Kramer et al. 1980; Krasiński 1983; Dąbrowski 1993). In these models the energy density depends just on the cosmic time, similar to the Friedmann models, but the pressure is a function of both spatial coordinates and a time coordinate; hence the models are usually referred to as ‘inhomogeneous pressure universes’. Essentially this means that there is a non-gravitational force throughout the entire universe which causes all particles not to move along the geodesics then experiencing acceleration. We suspect that such a force might be related to a vacuum energy density similar to the effect of a cosmological constant or cosmic string background which would be spatially dependent (e.g., Vilenkin 1985) and the standard energy conditions of Hawking and Penrose might be violated (cf. Hawking & Ellis 1973). However realistic these models might be, our primary goal here is to draw attention to the entire class of inhomogeneous models which could be a useful alternative to Friedmann models in helping

to resolve the apparent incompatibility of measurements of the Friedmann cosmological parameters.

The reader interested in more generic models should be referred to the recent review by Krasiński (1993), as well as to some earlier papers concerning the most popular generalization of the Friedmann models such as the spherically symmetric Tolman Universes (Tolman 1934; Bondi 1947; Bonnor 1974). Their properties have been studied quite thoroughly in Hellaby & Lake (1984, 1985) and Hellaby (1987, 1988) and the observational relations for Tolman models were studied by Goicoechea & Martin-Mirones (1987), Moffat & Tatarski (1995) and quite recently by Humphreys, Maartens & Mavtravers (1997).

The outline of this paper is as follows. In Section 2 we reproduce the redshift-magnitude relations for the two Stephani models considered here, as recently derived in Dąbrowski (1995). In Section 3 we briefly describe the SNIa data of P97 and outline their method of data reduction – in particular their adoption of a luminosity–light curve shape correlation to correct the ‘raw’ estimates of the intrinsic peak luminosity of the SNIa. In Section 4 we fit these data to the redshift-magnitude relations of both Friedmann and Stephani models and thus obtain best-fit values for the model parameters. We then discuss the results of these fits and compare the age of the Universe given by the best-fit model parameters in the Friedmann and Stephani cases. Finally in Section 5 we summarise our conclusions.

2 THE REDSHIFT-MAGNITUDE RELATION FOR INHOMOGENEOUS PRESSURE MODELS

Recently Dąbrowski (1995) has considered the redshift-magnitude relation for Stephani universes. Two exact cases were presented and the predicted relations were plotted for a range of different parameter values. The relations were defined following the method of Kristian & Sachs (1966), of expanding all relativistic quantities in power series and truncating at a suitable order. Approximate formulae, to first order in redshift z , for Model I and Model II respectively were given by

$$m_B = M_B + 25 + 5 \log_{10} \left[cz \left(\frac{a\tau_0^2 + b\tau_0 + d}{2a\tau_0 + b} \right) \right] + 1.086 \left[1 + 2a \frac{(a\tau_0^2 + b\tau_0 + d)}{(2a\tau_0 + b)^2} \right] z \quad (2)$$

and

$$m_B = M_B + 25 - 5 \log_{10} \frac{2}{3\tau_0} + 5 \log_{10} cz + 1.086 \left(\frac{1}{2} + \frac{9}{8} c^2 \alpha \tau_0^{\frac{4}{3}} \right) z, \quad (3)$$

which are essentially equations (5.6) and (5.10) respectively of Dąbrowski (1995) *. Here m_B and M_B denote apparent and absolute magnitude respectively in the B band, τ_0 denotes the age of the Universe and $c = 3 \times 10^5 \text{ km s}^{-1}$ is the velocity of light. The constants a, b and d are parameters

* but written now for B band observations, which are the case under study in this paper

of Model I and α is a parameter of Model II. Convenient units for these parameters are: $[a] = \text{km}^2 \text{s}^{-2} \text{Mpc}^{-1}$, $[b] = \text{kms}^{-1}$, $[d] = \text{Mpc}$ and $[\alpha c^2] = (\text{kms}^{-1} \text{Mpc})^{-\frac{1}{3}}$. From the definition of the acceleration scalar (c.f. Dąbrowski 1995) we conclude that the parameters which relate directly to the non-uniformity of the pressure are a in Model I and α in Model II.

The models considered here are spherically symmetric, which means that we can have both centrally placed and non-centrally placed observers. For simplicity the redshift-magnitude relations reproduced above correspond to a centrally placed observer. Dąbrowski (1995) also derived relations for the case of a non-centrally placed observer which, although more general, introduced several additional free parameters. The main difference in this more general case is that the apparent magnitude depends on the position of the source in the sky, and renders comparison with the Friedmann case more complicated. We thus consider only centrally placed observers in this paper.

Note that these formulae are truncated at first order in z and thus would become increasingly inaccurate if applied to redshifts greater than or equal to unity. Since the redshifts of the P97 preliminary data extend only to $z \sim 0.5$ we proceed with the first-order expressions, and will also use the first-order expression for Friedmann models when comparing the fits. In future work, as the database of high redshift SNIa grows, we will extend the approximate redshift-magnitude relations to higher order, as required.

The reader is referred to Dąbrowski (1995) for a detailed discussion of the derivation of the above formulae. Note, however, that for Model I the expression for the generalised scale factor, $R(\tau)$, as a function of cosmic time, τ , is given by (eq. 2.11 of Dąbrowski 1995)

$$R(\tau) = a\tau^2 + b\tau + d. \quad (4)$$

Thus, requiring that $R(\tau) \rightarrow 0$ as $\tau \rightarrow 0$ (i.e. setting the origin of our time coordinate at the Big Bang) demands that d is identically zero. We will therefore assume $d = 0$ throughout the rest of this paper, but otherwise will regard the remaining parameters of Models I and II essentially as free parameters.

3 THE SNIa OBSERVATIONS OF PERLMUTTER ET AL. (1997)

Type Ia supernovae are thought to be the result of the thermonuclear disruption of a white dwarf star which has accreted sufficient matter from a binary companion to reach the Chandrasekhar mass limit. For several decades they have been considered as suitable (nearly) standard candles for the testing of cosmological models because of the relatively small dispersion of their luminosity function at maximum light and the fact that they are observable at very great distances. In recent years the Hubble diagram of SNIa has been used by a number of authors to obtain estimates of the Hubble constant (c.f. Riess, Press & Kirshner 1996; Hamuy et al. 1995, 1996; Branch et al. 1996) and the motion of the Local Group (Riess, Press & Kirshner 1995). P97 consider the redshift-magnitude relation of SNIa at high redshift, observed by the ‘Supernova cosmology project’, as a means of

constraining q_0 . Their observing strategy, is designed to detect ‘batches’ of SNIa, virtually on a scheduling basis, by a sequence of intensive searches close to new moon. Their preliminary results present the analysis of seven SNIa in the redshift range $0.35 < z < 0.45$ with a further 11 SNIa detected and awaiting reduction. The SNIa were observed in the R band, with some additional photometry in the I band; in all cases the CCD photometry ensured good coverage of the light curve shape and a well-defined maximum light. After application of the K correction, light observed in the R band corresponded to radiation emitted in the B band.

In all of the above applications to estimate cosmological parameters SNIa were not treated as precise standard candles – i.e. the absolute magnitude at maximum light of each calibrating SNIa was not regarded as lying exactly at the peak of the SNIa luminosity function – but instead the peak luminosity of each SNIa was constrained using a second parameter related to the decline rate of the light curve. Evidence for the existence of such a correlation is quite convincing, although it is parameterised in different ways by different authors. Hamuy et al. (1995, 1996) used the parameter Δm_{15} , the change in apparent magnitude over the first 15 days after maximum light, to characterise the decline rate; Riess, Press & Kirshner (1995, 1996) introduced a ‘linear correction template’ designed to relate the differences in the peak luminosity of SNIa to differences in their light curve shape over the entire outburst. The approach adopted by Perlmutter et al. is in some sense a hybrid of the above two methods in that it uses information over the whole light curve but characterises differences in peak magnitude of SNIa in terms of a single parameter. Their procedure is to compare the light curve with that of a Leibundgut ‘normal template’ SNIa (Leibundgut et al. 1991), allowing the time axis of the observed data to be multiplied by a ‘stretch factor’ which is fitted from the data. Having established from nearby calibrating SNIa a relation between the stretch factor and the difference in magnitude from the normal template at maximum light, Perlmutter et al. correct their distant SNIa to the apparent magnitude which they would have if they followed the standard template light curve.

Following Table 1 of P97, Table 1 lists the redshifts and apparent B band magnitudes, both before and after correction by the stretch factor, for the seven SNIa. As is discussed in detail by P97, the light curves of SN1992bi and SN1994F displayed stretch factors which lay outside the range observed for the local calibrating SNIa; in the following section we, therefore, compare Friedmann and Stephani models using the corrected magnitudes for only the remaining five SNIa. The photometric magnitude errors quoted in Table 1 are in all cases as given in P97.

4 COMPARISON OF THE DATA WITH FRIEDMANN AND STEPHANI MODELS: RESULTS AND DISCUSSION

4.1 Friedmann Models

Figure 1 shows the Hubble diagram of the P97 SNIa. In Figure 1a the uncorrected B band apparent magnitudes are plotted against $\log(cz)$ for all seven SNIa, while in Figure 1b the corrected apparent magnitudes are shown for the five

SNIa	z	m_B	$m_{B,corr}$
SN 1992bi*	0.458	22.71 ± 0.09	23.26 ± 0.24
SN 1994H	0.374	21.92 ± 0.06	22.08 ± 0.11
SN 1994al	0.420	22.84 ± 0.13	22.79 ± 0.27
SN 1994F*	0.354	22.61 ± 0.18	21.80 ± 0.69
SN 1994am	0.372	22.27 ± 0.07	22.02 ± 0.14
SN 1994G	0.425	22.31 ± 0.16	22.36 ± 0.35
SN 1994an	0.378	22.48 ± 0.07	22.01 ± 0.33

Table 1. Redshifts and apparent B band magnitudes, before and after correction for the luminosity–light curve shape correlation, for the seven SNIa of P97. The SNIa marked with an asterisk had correction factors which lay outside the range calibrated by local SNIa.

SNIa whose stretch factors were within the range found for the calibrating sample of Hamuy et al. (1996). The error bars are calculated following P97, by adding in quadrature the photometric error on each apparent magnitude (as given in Table 1), the dispersion, σ_M , and the zero-point uncertainty, σ_{ZP} , of the best-fit linear relation derived from the low redshift calibrators. For the uncorrected data $\sigma_M = 0.26$ and $\sigma_{ZP} = 0.03$, while for the corrected data $\sigma_M = 0.17$ and $\sigma_{ZP} = 0.05$. Also shown on these diagrams are the magnitude-redshift relations for a Friedmann model with $q_0 = -0.5$ (dotted), $q_0 = 0.0$ (dot-dash), $q_0 = 0.5$ (solid) and $q_0 = 1.0$ (dashed). These relations are obtained via the equation

$$m_B = M_B + 5 \log_{10} cz + 1.086(1 - q_0)z, \quad (5)$$

where

$$M_B = M_B - 5 \log_{10} H_0 + 25, \quad (6)$$

with the corresponding expression for the corrected B band magnitudes. Following P97 we adopt $M_B = -3.17 \pm 0.03$ and $M_{B,corr} = -3.32 \pm 0.05$.

From Figures 1a and 1b it is clear that the data, although small in number, are already seen to be more consistent with positive values of q_0 , and the best-fit value of q_0 would appear to be around $q_0 = 0.5$. We construct the (reduced) chi-squared statistic:-

$$\chi^2 = \frac{1}{n-1} \sum_{i=1}^n \left[\frac{m_B^{\text{obs}}(i) - m_B^{\text{pred}}(i)}{\sigma(i)} \right]^2, \quad (7)$$

where n is the number of SNIa, $m_B^{\text{obs}}(i)$ and $\sigma(i)$ are respectively the observed B band apparent magnitude and error estimate (i.e. the error bar of Figures 1a and 1b) of the i^{th} SNIa, and $m_B^{\text{pred}}(i)$ is the predicted B band apparent magnitude of the i^{th} SNIa, for a given value of q_0 , derived from equation 5 (or its equivalent for the corrected magnitudes). From equations 5 and 7 it follows that \hat{q}_0 , the maximum likelihood (equivalently minimum χ^2) estimate of q_0 , is given by:-

$$\hat{q}_0 = - \left[\sum_{i=1}^n \frac{x_i y_i}{\sigma^2(i)} \right] \left[\sum_{i=1}^n \frac{x_i^2}{\sigma^2(i)} \right]^{-1}, \quad (8)$$

where

$$x_i = 1.086z(i) \quad (9)$$

and

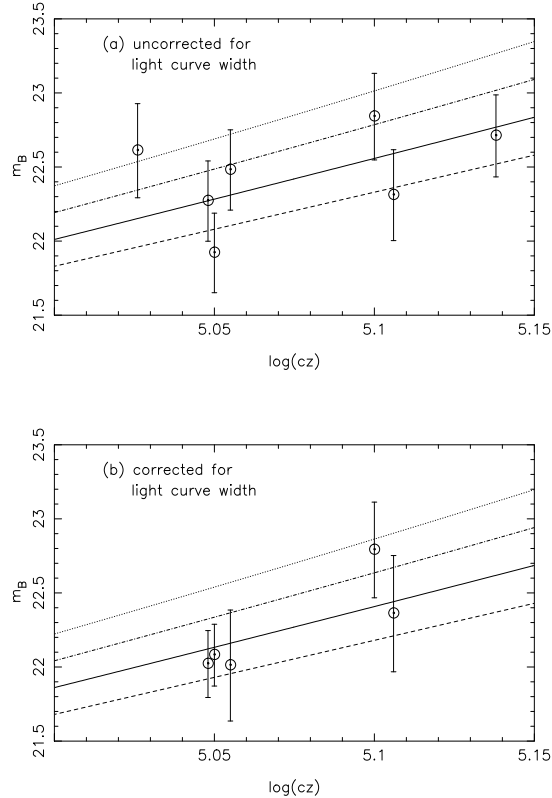


Figure 1. B band apparent magnitudes plotted against $\log(cz)$ for the SNIa of P97. Figure 1a shows uncorrected magnitudes for all seven SNIa; figure 1b shows corrected magnitudes for the five SNIa whose stretch factors were within the range found for the calibrating sample of Hamuy et al. (1996). The error bars are calculated following P97. Also shown are the magnitude-redshift relations for a Friedmann model with $q_0 = -0.5$ (dotted), $q_0 = 0.0$ (dot-dash), $q_0 = 0.5$ (solid) and $q_0 = 1.0$ (dashed).

$$y_i = m_B^{\text{obs}}(i) - M_B - 5 \log cz(i) - 1.086z(i). \quad (10)$$

Substituting the appropriate values from Table 1 we find that $\hat{q}_0 = 0.48$ for the uncorrected magnitudes and $\hat{q}_0 = 0.50$ for the corrected magnitudes. Thus we see that applying the magnitude corrections has negligible effect on the best-fit value of q_0 for the P97 data.

Figure 2 shows the value of χ^2 , for $-0.5 < q_0 < 1$, both for the uncorrected (solid line) and corrected data (dashed line). We can see from this figure that the corrected data consistently give a slightly better fit to a Friedmann model than the uncorrected data for a wide range of values of q_0 . Both the uncorrected and corrected data give an acceptable fit over the range $0 < q_0 < 1$ (and in fact over a somewhat wider range for the corrected data) but both give a poor fit for large negative values of q_0 .

Table 2 quantifies the goodness of fit of the SNIa data to a number of Friedmann models with different values of the cosmological parameters Ω_m , Ω_Λ , and the age of the universe, t_0 – all for a Hubble constant $H_0 = 65 \text{ km s}^{-1} \text{ Mpc}^{-1}$. Column (3) shows the corresponding value of q_0 , calculated from equation 1. Column (5) gives the reduced χ^2 of the fit to all seven SNIa, while column (6) gives the reduced χ^2 obtained using the five SNIa with corrected magnitudes.

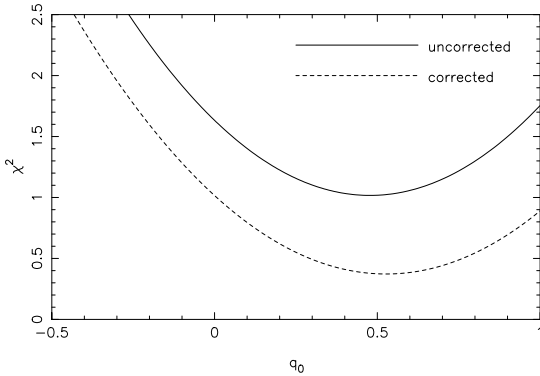


Figure 2. The value of χ^2 , for $-0.5 < q_0 < 1$, both for the uncorrected (solid line) and corrected data (dashed line).

Ω_m	Ω_Λ	q_0	t_0 (Gyr)	χ^2	χ^2_{corr}
1.0	0.0	0.5	10.0	0.87	0.37
0.5	0.0	0.25	11.3	0.99	0.55
0.5	0.5	-0.25	12.5	2.09	1.77
0.3	0.0	0.15	12.2	1.12	0.70
0.3	0.7	-0.55	14.5	3.31	3.06
0.3	0.15	0.0	12.9	1.40	1.02
0.2	0.0	0.1	12.7	1.20	0.79
0.2	0.8	-0.7	16.2	4.07	3.86
0.2	0.1	0.0	13.4	1.40	1.02

Table 2. Goodness of fit, expressed as a reduced χ^2 , of the SNIa data to Friedmann models with different combinations of Ω_m and Ω_Λ . Column (3) gives the corresponding value of q_0 and column (4) the age, t_0 , of the universe assuming $H_0 = 65 \text{ km s}^{-1} \text{ Mpc}^{-1}$. Columns (5) and (6) respectively give the reduced χ^2 of the fit to all seven SNIa and to the five SNIa with corrected magnitudes.

It is clear from Table 2 that one cannot obtain, with $H_0 \simeq 65 \text{ km s}^{-1} \text{ Mpc}^{-1}$, an acceptable fit to either the corrected or uncorrected data and at the same time ensure an age of the universe in excess of 14 Gyr.

4.2 Stephani Model II

We now compare the SNIa data with the predicted magnitude-redshift relations of the Stephani models. We consider first Model II, and the relation given by equation 3. If we compare equations 3 and 5 we see that in the limit as $z \rightarrow 0$ these equations are identical if and only if

$$\tau_0 = \frac{2}{3} H_0^{-1}. \quad (11)$$

In other words for nearby SNIa, Stephani Model II predicts the same linear redshift-magnitude relation as do Friedmann models, and with an age of the universe equal to two thirds times the inverse of the Friedmann Hubble constant. This is precisely the age of a Friedmann universe which is flat with a zero cosmological constant. In particular, if $H_0 \sim 65 \text{ km s}^{-1} \text{ Mpc}^{-1}$ then *independent of the value of the parameter, α* , the age of the universe τ_0 in Model II is approximately 10 Gyr, which certainly appears to be too low to be consistent with astrophysical age determinations. Hence it

would seem that Model II is not particularly useful in resolving the current age conflict since the age is inextricably linked to the value of the Friedmann Hubble constant: as soon as the latter is specified then so too is the age of Model II.

The link between the magnitude-redshift relation for Model II and the Friedmann case is, nonetheless, interesting for the following reason. Note that equation 3 may be rewritten as

$$\begin{aligned} m_B &= M_B + 25 - 5 \log_{10} \frac{2}{3\tau_0} + 5 \log_{10} cz \\ &+ 1.086(1 - q_0)z, \end{aligned} \quad (12)$$

where

$$q_0 = \left(\frac{1}{2} - \frac{9}{8} c^2 \alpha \tau_0^{\frac{4}{3}} \right), \quad (13)$$

which means that for any given age of the universe, τ_0 , we can choose the parameter, α , so that the magnitude-redshift relation for Model II is identical in form to equation 5, with $\tau_0 = \frac{2}{3} H_0^{-1}$. The crucial difference is that, whereas in the Friedmann case with $\Lambda = 0$, equation 11 implies that $q_0 = 0.5$, in the Stephani case we still retain the freedom to specify a relation which is equivalent to *any* value of q_0 by suitable choice of α . In particular, then, by choosing $\alpha < 0$ we can obtain a magnitude-redshift relation which corresponds to a Friedmann model with $q_0 > 0.5$. While in the Friedmann case this would imply an age of the universe $\tau_0 < \frac{2}{3} H_0^{-1}$, in the case of Model II we still have $\tau_0 = \frac{2}{3} H_0^{-1}$. Model II would, therefore, be of considerable interest if SNIa (or other) observations were to suggest that $q_0 > 0.5$, which, as can be seen from Figure 1, certainly cannot be ruled out on the basis of the P97 data alone. As an illustrative (if somewhat extreme) example, consider the case where $\Omega_m = 2$ and $\Omega_\Lambda = 0$, so that $q_0 = 1$ for the Friedmann model. As can be seen from equation 13 the Friedmann and Model II magnitude-redshift relations are identical when

$$\alpha = -\frac{4}{9} c^{-2} \tau_0^{-\frac{4}{3}}. \quad (14)$$

Whereas the age of the Friedmann model with $q_0 = 1$ would be reduced by about 15% compared with the Einstein de Sitter age (i.e. $\tau_0 \simeq 0.57 H_0^{-1}$), for the Stephani Model II we still have $\tau_0 = \frac{2}{3} H_0^{-1}$. Although the scenario of $q_0 > 0.5$ appears highly unlikely, in view of a variety of other observations of large scale structure and CMBR anisotropies, this serves as an interesting example of how the Stephani models can be compatible with high redshift observations over a larger region of parameter space than Friedmann models.

4.3 Stephani Model I

One of the reasons why Model II is not particularly useful as an extension of the Friedmann case is that the effect of the non-uniform pressure (manifest via the parameter α) only becomes apparent at high redshift. The situation with Stephani Model I is different, however. We can see from equation 2 that the effect on the magnitude-redshift relation of the non-uniform pressure parameters a and b is immediate. In particular, therefore, even at low z Model I does not in general reduce trivially to a specific Friedmann case.

Note that we can eliminate one of the parameters a

and b from Model I since (provided $d = 0$) we can rewrite equation 2 to depend only upon their ratio, $\Delta \equiv b/a$.[†] Thus

$$\begin{aligned} m_B &= M_B + 25 + 5 \log_{10} \left[cz \left(\frac{\tau_0^2 + \Delta \tau_0}{2\tau_0 + \Delta} \right) \right] \\ &+ 1.086 \left[1 + 2 \frac{(\tau_0^2 + \Delta \tau_0)}{(2\tau_0 + \Delta)^2} \right] z. \end{aligned} \quad (15)$$

As a means of estimating what range of values of Δ and τ_0 will give an acceptable fit to the P97 data it is useful to note further that we may recast equation 15 in the form

$$\begin{aligned} m_B &= M_B + 25 + 5 \log_{10} cz - 5 \log_{10} \tilde{H}_0 \\ &+ 1.086(1 - \tilde{q}_0)z, \end{aligned} \quad (16)$$

where

$$\tilde{H}_0 = \frac{2\tau_0 + \Delta}{\tau_0^2 + \Delta\tau_0} \quad (17)$$

and

$$\tilde{q}_0 = -2 \frac{\tau_0^2 + \Delta\tau_0}{(2\tau_0 + \Delta)^2}. \quad (18)$$

Equation 16 now takes the same functional form as equation 5, as was similarly pointed out in Dąbrowski (1995), with \tilde{H}_0 and \tilde{q}_0 replacing H_0 and q_0 . We can think of \tilde{H}_0 (which is one third of the expansion scalar Θ of the model) and \tilde{q}_0 as a generalised Hubble parameter and deceleration parameter which are related to the age of the universe in a different way from the Friedmann case. The key question of interest here is therefore whether one can construct generalised parameters, \tilde{H}_0 and \tilde{q}_0 , which are in good agreement with the P97 data but which correspond to a value of τ_0 which exceeds that Friedmann age with $H_0 = \tilde{H}_0$ and $q_0 = \tilde{q}_0$. The fact that we can write the Model I redshift-magnitude relation in the form of equation 16 confirms, however, that our choices of τ_0 and Δ are certainly *not* arbitrary. Combinations of τ_0 and Δ which give a large negative value of \tilde{q}_0 , for example, would clearly be incompatible with the SNIa Hubble diagram – just as was the case for Friedmann models with $q_0 < 0$. One approach to fitting the parameters of Model I could be to make use of equation 16 and first fix the values of \tilde{H}_0 and \tilde{q}_0 to be equal to their best-fit Friedmann counterparts: i.e. $\tilde{H}_0 \sim 65$ and $\tilde{q}_0 \sim \frac{1}{2}$. One could then explore which values of τ_0 and Δ give rise to these fixed values of \tilde{H}_0 and \tilde{q}_0 . This approach is unnecessarily restrictive, however, since we are primarily interested in maximising τ_0 while still keeping an *acceptable* fit to the SNIa data. Having determined optimal values of τ_0 and Δ in this sense, we can then compute \tilde{H}_0 and \tilde{q}_0 as a consistency check.

In order to estimate the parameters τ_0 and Δ we construct the reduced chi-squared statistic:-

[†] One should emphasize that there are singularities of pressure in the model which may appear throughout the universe for some values of the radial coordinate r if $b^2 > 1$. Fortunately, our analysis based on the value of Δ rather than just on b allows us to choose a broad range of parameters for which these singularities can be fully avoided or at least moved away from the observer at $r = 0$.

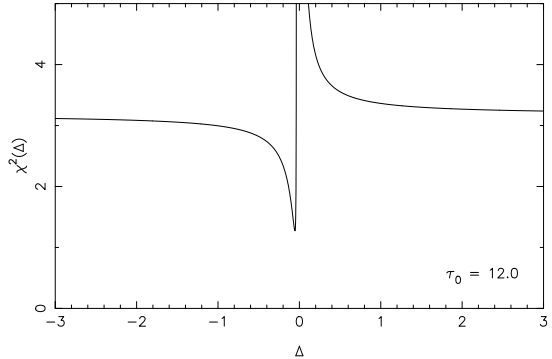


Figure 3. Plot of χ^2 as a function of Δ , for a fixed value of $\tau_0 = 12$ Gyr, obtained from a comparison of the apparent magnitudes predicted by Stephani Model I with the uncorrected magnitudes of P97.

$$\chi^2 = \frac{1}{n-2} \sum_{i=1}^n \left[\frac{m_B^{\text{obs}}(i) - m_B^{\text{pred}}(i; \tau_0, \Delta)}{\sigma(i)} \right]^2, \quad (19)$$

where n is the number of SNIa and $m_B^{\text{pred}}(i; \tau_0, \Delta)$ is obtained for the i^{th} SNIa from equations 16, 17 and 18. We determine M_B in equation 16 from Hamuy et al. (1996), adopting their best-fit value of $H_0 = 63.1 \text{ km s}^{-1} \text{ Mpc}^{-1}$ determined from four local calibrating SNIa. Thus,

$$M_B \equiv \mathcal{M}_B + 5 \log H_0 - 25 = -19.17 \pm 0.03 \quad (20)$$

and

$$M_{B,\text{corr}} \equiv \mathcal{M}_{B,\text{corr}} + 5 \log H_0 - 25 = -19.32 \pm 0.05. \quad (21)$$

The dependence of equation 19 on τ_0 and Δ is highly non-linear, making a plot of the surface $z = \chi^2(\tau_0, \Delta)$ difficult to interpret. We therefore consider slices through this surface. Figure 3 shows χ^2 as a function of Δ for $\tau_0 = 12$ Gyr, using the uncorrected magnitudes of all the P97 SNIa. The behaviour of χ^2 is seen to be rapidly varying for values of Δ around zero, but is essentially asymptotically flat for $|\Delta| > 1$. For $\Delta > -0.5$ the value of χ^2 begins to drop steadily from its ‘plateau’ level to reach a minimum value at $\Delta \simeq -0.055$, before then rising very steeply as Δ increases further. By $\Delta \simeq 0.5$ the curve has fallen again to a new, asymptotically flat, level slightly higher than that for $\Delta < -0.5$. A very similar curve is obtained for the corrected magnitudes.

We can understand the behaviour of χ^2 for small values of Δ by considering the behaviour of \tilde{H}_0 and \tilde{q}_0 in equations 17 and 18. We see that when $\Delta = -2\tau_0$ we have $\tilde{H}_0 = 0$ and $\tilde{q}_0 \rightarrow \infty$,[‡] so that χ^2 is singular. It therefore follows that

[‡] This is a special situation, and moreover one which contradicts the observations since it would mean that the present day is exactly the turning point of the cosmic evolution. Following eqs. (57a)-(57b) of Dąbrowski (1993) the energy density at the moment $\tau_0 = -\Delta/2$ is $\varrho = 48a^2/b^4$ and the pressure $p = \varrho\{-1/3 + 2/3[b^2r^2/4 + (1 - b^2)r^2]\}$. In the Friedman limit $a \rightarrow 0_-$ ($a < 0$, if one wants $R(\tau) > 0$) we have $\tau_0 \rightarrow \infty$, and $p = \varrho = 0$ which is an everlasting, empty and static universe – a subcase of little or no physical interest.

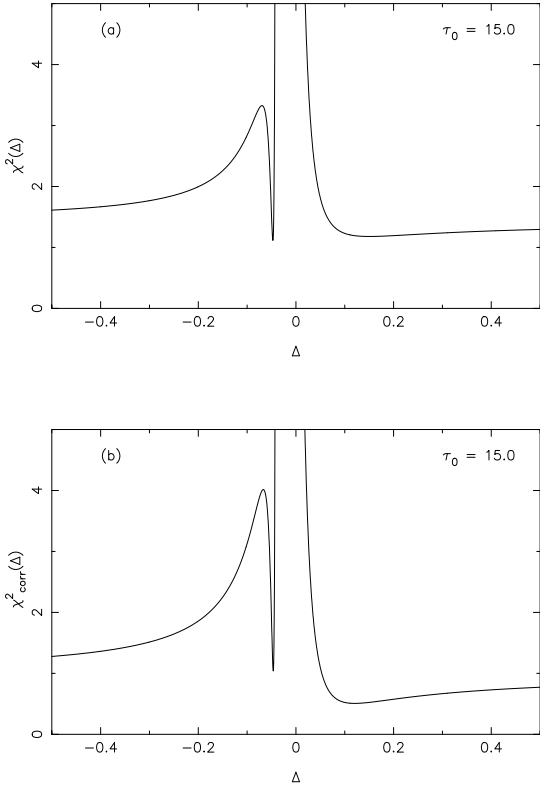


Figure 4. Plot of χ^2 as a function of Δ , for a fixed value of $\tau_0 = 15$ Gyr, obtained from a comparison of the apparent magnitudes predicted by Stephani Model I with the magnitudes of P97. Figure 4a is for the uncorrected magnitudes and figure 4b is for the corrected magnitudes.

for $\tau_0 = 12$ Gyr = 12.24×10^{-3} sMpc km^{-1} a singular value of χ^2 occurs when $\Delta \simeq -0.024$ sMpc km^{-1} , as observed, and χ^2 will vary very rapidly for values of Δ close to this value.

Figures 4a and 4b show plots of χ^2 as a function of Δ but now with $\tau_0 = 15$ Gyr, for the corrected and uncorrected magnitudes respectively. A narrower range of values of Δ is shown, in order to better illustrate the behaviour of χ^2 close to the origin. We find that χ^2 again tends to infinity when $\Delta = -2\tau_0$, and is asymptotically flat for $|\Delta| \gg 0$. Note that the local minimum value of χ^2 for $\Delta < 0$ is now in a very narrow ‘valley’, bordered by the singular value at $\Delta = -2\tau_0$ on one side and a local maximum value on the other side, and – in the case of the corrected magnitudes – is also not the global minimum value.

Figures 5a and 5b show plots of χ^2 as a function of τ_0 for $\Delta = 1.0$, for the uncorrected and corrected magnitudes respectively. We see that Model II gives a good fit to the P97 data for τ_0 in the range 13 to 15 Gyr. Figures 6a and 6b show the values of \tilde{H}_0 and \tilde{q}_0 respectively as a function of τ_0 for $\Delta = 1.0$. Also shown on figures 6a and 6b are the best-fit values of $H_0 = 63.1$ kms $^{-1}$ Mpc $^{-1}$ and $q_0 = 0.5$ obtained from Hamuy et al. (1996) and P97 respectively. Note from figure 6b that \tilde{q}_0 is almost independent of τ_0 , for τ_0 in the range shown, and that $\tilde{q}_0 \simeq 0$. The dependence of \tilde{H}_0 on τ_0 is rather more pronounced, however: $\tilde{H}_0 \sim 65$ for τ_0 in the

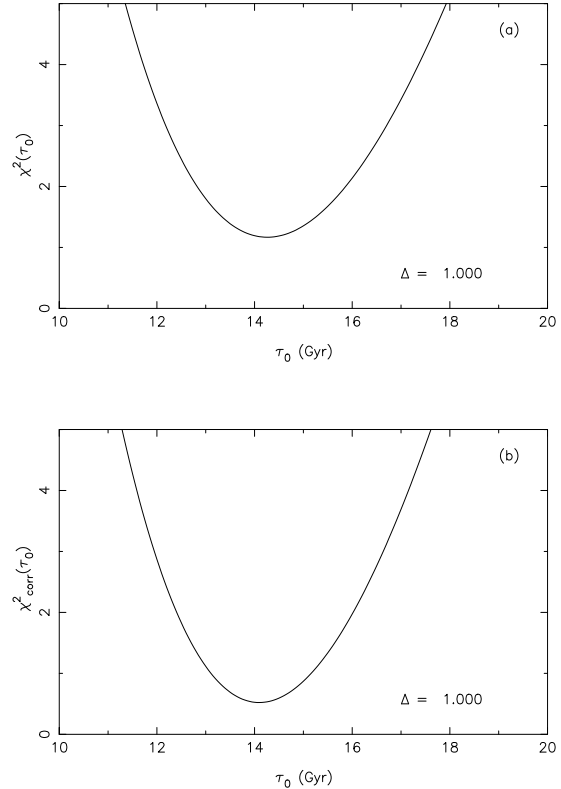


Figure 5. Plot of χ^2 as a function of τ_0 , for a fixed value of $\Delta = 1.0$, obtained from a comparison of the apparent magnitudes predicted by Stephani Model I with the magnitudes of P97. Figure 5a is for the uncorrected magnitudes and figure 5b is for the corrected magnitudes.

range 15 to 16 Gyr, with the curve intercepting the Hamuy et al. (1996) value at $\tau_0 \simeq 15.7$ Gyr.

The behaviour of \tilde{H}_0 and \tilde{q}_0 in figures 6a and 6b makes sense when we consider the form of equations 17 and 18 for $\tau_0 \ll \Delta$. To first order in τ_0/Δ these reduce to

$$\tilde{H}_0 = \frac{1}{\tau_0} \left(1 + \frac{\tau_0}{\Delta} \right) \quad (22)$$

and

$$\tilde{q}_0 = -2 \frac{\tau_0}{\Delta}. \quad (23)$$

Thus we see that as $\tau_0/\Delta \rightarrow 0$, $\tilde{H}_0 \rightarrow \tau_0^{-1}$ and $\tilde{q}_0 \rightarrow 0$.

The usefulness of Model II is now apparent: the age of the universe is increased by 50% compared with the Einstein de Sitter case, in the limit where $\tau_0/\Delta \rightarrow 0$, which gives $\tau_0 = 15$ Gyr (compared with only 10 Gyr) for $H_0 \sim 65$. Although in this limit the value of $\tilde{q}_0 \rightarrow 0$ (compared with $q_0 = 0.5$ for an Einstein de Sitter universe) we can see from figures 1a and 1b and table 2 that $q_0 = 0$ still gives an acceptable fit to the uncorrected and corrected data. For a Friedmann model with $q_0 = 0$ the age of the universe depends on the matter density, Ω_m , but it is clear from table 2 that – even with $\Omega_m = 0.3$ – the age of the Universe would still be less than 13 Gyr in the Friedmann case. Very similar behaviour is found for $\Delta = -1.0$, with the corrected and uncorrected data again being well-fitted by $\tau_0 \sim 15$ Gyr,

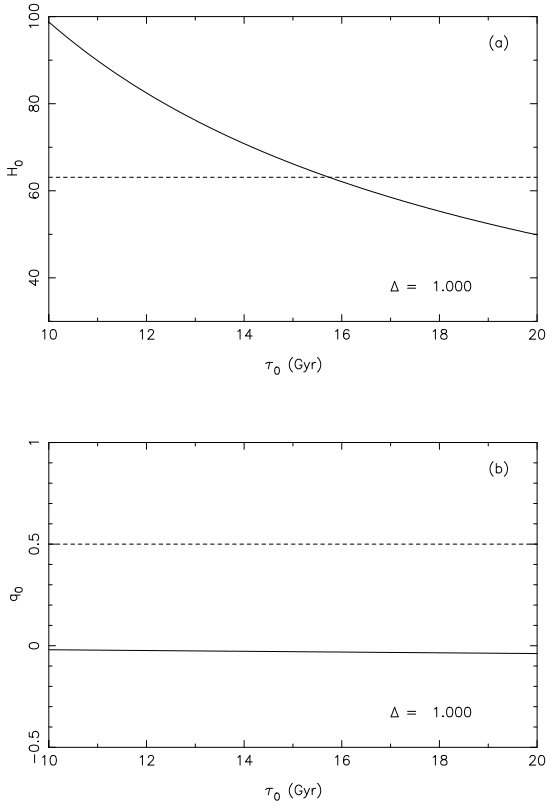


Figure 6. Plot of the effective Friedmann parameters, \tilde{H}_0 and \tilde{q}_0 , as a function of τ_0 , for a fixed value of $\Delta = 1.0$. Dotted lines indicate the best-fit Friedmann for H_0 (Figure 6a) from Hamuy et al. (1996) and q_0 (Figure 6b) from P97.

although since from equation 23 we now have $q_0 \rightarrow 0$ from above, the fit to the P97 data for $\tau_0 \sim 15$ Gyr is in fact slightly better than when $\Delta = 1.0$.

We have emphasised the asymptotic behaviour of $|\Delta|$, which is already well-represented by $|\Delta| = 1$, in order to make clear that the usefulness of Model II is a fairly robust result and is not too sensitive to the exact values of the Model II parameters, a and b , chosen. In fact one can obtain a good fit – with $\tau_0 \sim 15$ Gyr, $\chi^2 \sim 1$ and $\tilde{H}_0 \sim 65$ – to both the corrected and uncorrected data for all $|\Delta| > 0.3$. As was the case in the illustrative example shown in figure 6b, most of these fits give $\tilde{q}_0 \sim 0$, in accordance with equation 23. By ‘fine tuning’ the parameters of Model II, however, one can obtain fits which give significant positive values of \tilde{q}_0 , and which are therefore in much closer agreement with the best-fit Friedmann value of $q_0 = 0.5$ obtained from the P97 data. In such cases there is still a significant difference between the age of the universe in the Friedmann and Stephani models. Some examples are given in table 3. The final two columns of table 3 show the age, τ_F , of the universe in a Friedmann model with $\Lambda = 0$ and with $\Omega_m + \Omega_\Lambda = 1$ respectively.

Some general trends are evident from table 3. We see that as τ_0 increases and Δ becomes more negative, the values of \tilde{H}_0 and \tilde{q}_0 are both reduced and the goodness of fit to the corrected and uncorrected data deteriorates. For $\tau_0 \geq 16$ Gyr, the goodness of fit quickly becomes unacceptably large: although by suitable choice of Δ one can ensure that \tilde{q}_0

remains positive, the value of \tilde{H}_0 also reduces and overall the fit deteriorates. Making $|\Delta|$ larger increases the value of \tilde{H}_0 and pushes \tilde{q}_0 close to zero, but does not significantly improve the goodness of fit.

It would seem that an age of $\tau_0 = 15$ Gyr represents the upper age limit from Model II with the P97 data. If subsequent analysis of larger samples of SNIa serve to tighten the limits on a positive value of \tilde{q}_0 , then this limiting age would be somewhat reduced. The important point to note, however, is that in this case the age limits on Friedmann models would *also* be reduced. As can be seen from table 3, a value of $\tilde{q}_0 \sim 0.5$ is well fitted by Model II with $\tau_0 = 13$ Gyr, which still represents an increase in the age of the universe of about 2.5 Gyr compared with a Friedmann model with either zero cosmological constant or critical density.

5 CONCLUSIONS

In this paper we have considered the two exact non-uniform pressure spherically symmetric Stephani universes, and have compared the redshift-magnitude relations derived for these models in Dąbrowski (1995) with the recent SNIa observations of P97. We have investigated the extent to which, by suitable choice of the Stephani model parameters, we may obtain good fits of the P97 data to the predicted redshift-magnitude relations but for universes which are older than their Friedmann counterparts.

We have found that the age of the universe in Stephani Model II is, in fact, independent of the model parameter, α , and is equal to the age of an Einstein de Sitter Friedmann model, i.e. $\tau_0 = \frac{2}{3}H_0^{-1}$. This model would be of considerable interest if the total density of the universe were greater than the critical density, since the age of the corresponding Friedmann model would then be *less* than the Einstein de Sitter age. Since there exists no compelling observational evidence to suggest that the universe is closed, however, Model II is of limited use as it would in general predict an age which was smaller than its Friedmann counterpart with the same value of the Hubble constant.

We have shown that Stephani Model I would be of considerably greater interest, however. We have found that the redshift-magnitude relation predicted for Model I can be expressed in terms of two parameters: the age, τ_0 , of the universe and the ratio, Δ of the two Stephani model parameters a and b . One can write the redshift-magnitude relation in exactly the same form as in the Friedmann case, introducing an effective Hubble parameter, \tilde{H}_0 , and deceleration parameter, \tilde{q}_0 , which are non-linear functions of Δ and τ_0 . We have shown that for a wide range of different values of Δ we can obtain good fits to the P97 data for a universe of age up to 15 Gyr, which is typically two or three Gyr greater than the corresponding Friedmann model. These fits are quite robust, requiring only that $|\Delta| > 0.3$. For small τ_0/Δ , the effective deceleration parameter, \tilde{q}_0 , is close to zero – a value which is certainly not as yet ruled out by the P97 data, although the fit to a value of $\tilde{q}_0 = 0.5$ is currently somewhat better. By some fine-tuning of the Model I parameters, one can obtain good fits with $\tilde{q}_0 \sim 0.5$ and $\tau_0 \sim 13$ Gyr. While an age of only 13 Gyr is probably still in conflict with astrophysical age determinations, the conflict is considerably worse for Friedmann models: the age of an $H_0 \sim 65$, $q_0 \sim 0.5$ critical

τ_0 (Gyr)	Δ	\tilde{H}_0	\tilde{q}_0	χ^2	χ^2_{corr}	$\tau_F(\Lambda = 0)$	$\tau_F(\Omega_m + \Omega_\Lambda = 1)$
13.0	-0.10	63.7	0.43	1.13	0.58	10.5	10.4
13.5	-0.12	63.0	0.34	1.18	0.69	11.1	10.7
14.0	-0.15	62.5	0.26	1.32	0.90	11.7	11.0
14.5	-0.20	62.0	0.19	1.53	1.19	12.3	11.3
15.0	-0.26	61.1	0.14	1.83	1.61	13.0	11.7
16.0	-0.35	58.1	0.11	2.89	3.04	14.1	12.4

Table 3. Fits of Stephani Model II universes with significantly positive values of \tilde{q}_0 to the P97 data. The final two columns show the age, τ_F , of the universe in a Friedmann model with $\Lambda = 0$ and with $\Omega_m + \Omega_\Lambda = 1$ respectively.

density Friedmann universe is only ~ 10 Gyr, and for closed models with $q_0 \sim 0.5$ the age is even smaller.

Thus, we find that Model I can give an age of the universe which is consistently and robustly between two and three Gyr older than the oldest acceptable open or flat Friedmann models.

In this paper we have considered only a particular class of inhomogeneous models, in order to illustrate their potential usefulness in addressing the apparent conflict between the observed values of the Friedmann model parameters. In future work we will extend our treatment to a wider class of non-Friedmann models and test their compatibility with the Hubble diagram of high-redshift objects and other cosmological observations. Such a comparison will be greatly enhanced by having larger samples of distant SNIa – a development which the modern observing strategies adopted by P97 and other groups will shortly provide.

6 ACKNOWLEDGEMENTS

The authors thank John Barrow for several useful discussions. MAH acknowledges the receipt of a PPARC personal research fellowship and a PPARC research assistantship. MPD acknowledges the support of the Royal Society and the hospitality of the Astronomy Centre at the University of Sussex.

REFERENCES

Bondi H., 1947, MNRAS, 107, 410
 Bonnor W. B., 1974, MNRAS, 167, 55
 Branch D., Fisher A., Baron E., Nugent P., 1996, ApJ, 470, 7L
 Chaboyer B., 1995, ApJ, 444, L9
 Dąbrowski M. P., 1993, Journ. Math. Phys., 34, 1447
 Dąbrowski M. P., 1995, ApJ, 447, 43
 Goicoechea L. J., Martin-Mirones J. M. 1987, A&A, 186, 22
 Gunn J. E., Oke J. B., 1975, ApJ, 195, 255
 Hamuy M., Phillips M. M., Maza J., Suntzeff N. B., Schommer R. A., Avilés R., 1995, AJ, 109, 1
 Hamuy M., Phillips M. M., Suntzeff N. B., Schommer R. A., Maza J., Avilés R., 1996, AJ, 112, 2398
 Hawking S. W., Ellis G. F. R., 1973, ‘The Large-Scale Structure of the Spacetime’, Cambridge University Press
 Hellaby C., Lake K., 1984, ApJ, 282, 1
 Hellaby C., Lake K., 1985, ApJ, 290, 381
 Hellaby C., 1987, Class. Quantum Grav., 4, 635
 Hellaby C., 1988, Gen. Rel. Grav., 20, 1203
 Hendry M. A., Tayler R. J., 1996, Contemp. Phys., 37, 263
 Humphreys N. P., Maartens R., Matravers D., 1997, ApJ, 477, 47.
 Kramer D., Stephani H., MacCallum M. A. H., Hertl E., 1980, ‘Exact Solutions of the Einstein Field Equations’, (CUP, Cambridge)
 Krasinski A., 1983, Gen. Rel. Grav., 15, 673
 Krasinski A., 1993, ‘Physics in an Inhomogeneous Universe’, Polish Research Committee and Department of Applied Mathematics, University of Cape Town, South Africa (Ed.)
 Kristian J., Sachs R. K., 1966, ApJ, 143, 379
 Leibundgut B., Tammann G. A., Cadonau R., Cerrito D., 1991, A&AS, 89, 537
 Liddle A. R., Lyth D. H., Viana P.T.P., White M., 1996, MNRAS, 283, 281
 Moffat J. W., Tatarski D.C., 1995, ApJ, 453, 17
 Peach J. V., 1970, ApJ, 159, 753
 Perlmutter S., et al., 1997, ApJ, in press, e-Print: astro-ph/9608192
 Postman M., 1997, to appear in ‘The Extragalactic Distance Scale’, eds. M. Livio, N. Panagia, M. Donohue (Cambridge)
 Riess A. G., Press W. H., Kirshner R. P., 1995, ApJ, 445, 91L
 Riess A. G., Press W. H., Kirshner R. P., 1996, ApJ, 473, 88
 Sandage A. 1988, ARA&A, 26, 561
 Schneider D. P., Gunn J. E., Hoessel J. G., 1983, ApJ, 264, 337
 Strauss M. A., Willick J. A., 1995, Physics Reports, 261, 271
 Tolman R. C., 1934, Proc. Nat. Acad. Sci., 20, 169
 Tonry J., 1993, in ‘Relativistic Astrophysics and Particle Cosmology’, eds. C. Akerlof, M. Srednicki (NY Acad. Sci.)
 Vilenkin A., 1985, Phys. Rep., 121, 265